IN-VENTO 2026
International Conference of the Italian Association for Wind Engineering
Bari, September 13th – 16th, 2026

BARI

Vortex-induced vibration of 1:2 subharmonic resonance: Phenomenon and modelling

Wei Cui [1], Yihan Xiao [1], Lin Zhao[1,2]

[1]*College of Civil Engineering, Tongji University, Shanghai, China, 200092*
[2]*College of Civil Engineering, Guangxi University, Nanning, Guangxi, China, 530004*

SUMMARY
As bridge spans increase, nonlinear wind-induced vibration phenomena occur frequently, among which nonlinear vortex-induced vibration (VIV) is prominent. Regarding VIV, it is generally believed that the phenomenon arises when the windspeed approaches the resonant windspeed and the vortex shedding frequency is close to the natural frequency of the bridge. However, some experimental results indicate that VIV can also occur when the wind speed is approximately half of the theoretical resonant wind speed. This paper attributes such phenomenon to subharmonic resonance vibration. Essentially, a double-frequency component existing in the flow field becomes close to the structural natural frequency, leading to the lock-in of flow frequency to the structural natural frequency and thus triggering VIV. Based on this hypothesis, a wake-oscillator model targeting 1:2 subharmonic vibration is established by modifying the classical Tamura wake-oscillator model. The proposed model achieves satisfactory fitting performance, which validates the conjecture presented in this study.

Keywords: vortex-induced vibration, subharmonic vibration, wake-oscillator model

1. Introduction

In recent years, VIV has occurred in several long-span bridges (Zhao et al., 2022). VIV is triggered by vortex-induced forces generated from vortex shedding after airflow passes through the bridge cross-sections. Main resonance-induced VIV occurs when the frequency of vortex-induced forces approaches the natural vibration frequency of the bridge. To simulate this resonance phenomenon, two major categories of semi-theoretical models have been established: single-degree-of-freedom models (SDOF models) and wake-oscillator models. When these models are adopted to simulate VIV, the vibration phenomenon only emerges near the resonant wind speed. However, partial experimental results reveal a new lock-in region happens in different section shapes when the wind speed is half of the resonant wind speed (Marra et al., 2015; Li et al., 2022; Shang et al., 2024), which corresponds to the 1:2 subharmonic resonance of VIV. This special phenomenon cannot be effectively considered by existing models. Based on experimental observations, this study proposes a reasonable hypothesis and establishes a theoretical model modified from the Tamura's wake-oscillator model to analyze test data, thereby revealing the mechanism underlying the 1:2 subharmonic resonance of VIV.

2. Wind tunnel test

The wind tunnel test results come from Marra's study (Marra et al., 2015). Wind tunnel test was conducted on a rectangular cross-section with a ratio of 4:1. As shown in

Figure 1, when Sc (Scruton number) is small, the section model experiences VIV within a wind speed range approximately half of the resonant wind speed. As shown in

Figure 1(b), before the occurrence of VIV, the vortex-shedding frequency is half of the resonant frequency, but when the subharmonic vibration is triggered, the vortex-shedding frequency turns into the structure resonant frequency.

a)

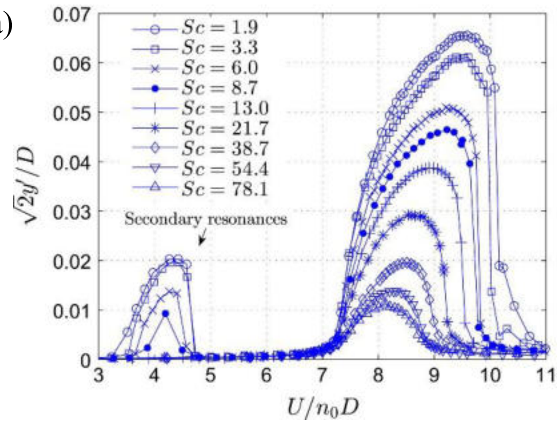

b)

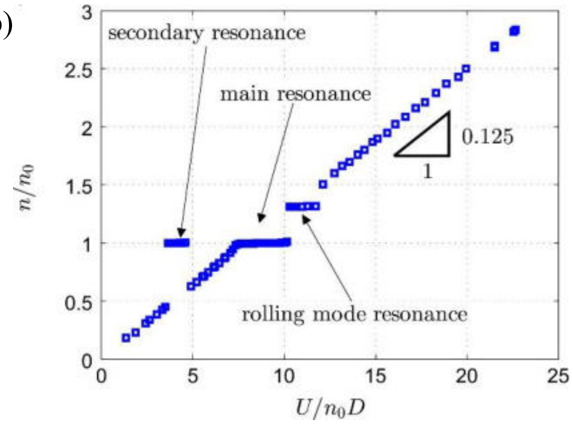

Figure 1 Results of wind tunnel test (a) Non-dimensional equivalent sinusoidal amplitudes of vibration at different reduced wind speeds for all the considered Sc. (b) non-dimensional dominant frequency of the velocity fluctuations in the wake.

3. Wake-oscillator model

3.1.Model establishment

The simplified result of the Tamura's wake oscillator model (Rigo et al., 2022) is as follows:

$$\ddot{\mathcal{Y}} + 2\xi\dot{\mathcal{Y}} + \mathcal{Y} = 2\epsilon M_0\mathcal{A}_1 \tag{1}$$
$$\ddot{\mathcal{A}}_1 + \epsilon\Omega(\mathcal{A}_1^2 - 1)\dot{\mathcal{A}}_1 + \Omega^2\mathcal{A}_1 = 2\epsilon\big(A_0\ddot{\mathcal{Y}} + A_1\Omega\dot{\mathcal{Y}}\big) \tag{2}$$

where $\mathcal{Y} = Y/\epsilon$, and Y is the dimensionless cross-flow structural motion. α_1 is the Angular position of the main wake that is the fundamental-frequency wake and $\mathcal{A}_1 = \alpha_1/\alpha^*$ with $\alpha^* = C_{L0}/2f$ to simplify the nonlinear term. The velocity ratio is $\Omega = \mathrm{U}/U_{cr}$ where U is the fluid velocity and $U_{cr} = f_0D/\mathrm{St}$ is the critical VIV velocity. The definitions of the other parameters can be found in (Rigo et al., 2022). Based on the previous section, it is assumed that the flow field contains a double-frequency modal component. VIV will occur when the double-frequency component is close to the structure frequency, at which point the double-frequency component is further excited by the structure, causing the dominant frequency of the flow field to equal to the structure frequency (as shown in Fig 1(a)).Then a double-frequency wake oscillator is used to simulate the above assumption. The subharmonic wake oscillator model is as follows:

$$\ddot{\mathcal{Y}} + 2\xi\dot{\mathcal{Y}} + \mathcal{Y} = 2\epsilon M_0 T\mathcal{A}_2 \tag{3}$$
$$\ddot{\mathcal{A}}_2 + 2\epsilon\Omega(\mathcal{A}_2^2 - 1)\dot{\mathcal{A}}_2 + 4\Omega^2\mathcal{A}_2 = 2\epsilon\big(T_1A_0\ddot{\mathcal{Y}} + T_2A_1\Omega\dot{\mathcal{Y}}\big) \tag{4}$$

$\mathcal{A}_2$ is the subharmonic wake that is the double-frequency wake. T represents the influence degree of the subharmonic wake on structural vibration, while T_1 and T_2 reflect the effects of structural acceleration and velocity on wake vibration, respectively. The theoretical frequency of the wake oscillator given by Eq.4 is twice that of Eq.2.When the wind speed is half the critical wind speed U_{cr}, the wake oscillation frequency from Eq.4 coincides with the structural vibration frequency, enabling the model to simulate the subharmonic VIV process.

3.2. Solution with averaging method

The averaging method is employed to solve the above nonlinear equations. By separating fast and slow variables on different time scales, the averaging method derives the evolution equations for the structure and wake oscillator amplitudes, yielding approximate solutions of the model and avoiding direct solution of complex nonlinear equations. The solutions to Eq. 1–Eq. 2 are presented in Eq. 5–Eq. 7. R_y is the amplitude of the structure, $R_{\mathcal{A}_1}$ is the amplitude of the main wake and β_1 is the phase difference between $R_{\mathcal{A}_1}$ and R_y where $\beta_1 = \beta_{\mathcal{A}_1} - \beta_y$.

$$\dot{R_y} = \epsilon M_0 R_{\mathcal{A}_1} \sin\beta_1 - \xi R_y \tag{5}$$

$$\dot{R_{\mathcal{A}_1}} = -\epsilon\Omega\left[\frac{R_{\mathcal{A}_1}^3}{8} - \frac{R_{\mathcal{A}_1}}{2}\right] + 2\epsilon\left[-A_0\xi R_y\cos\beta_1 + A_0\frac{R_y}{2}\sin\beta_1 + A_1\Omega\frac{R_y}{2}\cos\beta_1\right] \tag{6}$$

$$\dot{\beta_1} = 2\epsilon\left[-A_0\epsilon M_0 + A_0\xi\frac{R_y}{R_{\mathcal{A}_1}}\sin\beta_1 + A_0\frac{R_y}{2R_{\mathcal{A}_1}}\cos\beta_1 - A_1\Omega\frac{R_y}{2R_{\mathcal{A}_1}}\sin\beta_1\right] + \frac{\Omega^2-1}{2} + \epsilon M_0\frac{R_{\mathcal{A}_1}}{R_y}\cos\beta_1 \tag{7}$$

By the same way , the solutions to Eq.3–Eq.4 are presented in Eq.8–Eq.10. $R_{\mathcal{A}_2}$ is the amplitude of the subharmonic wake and β_2 is phase difference between $R_{\mathcal{A}_2}$ and R_y where $\beta_2 = \beta_{\mathcal{A}_1} - \beta_y$.

$$\dot{R_y} = -\xi R_y + \epsilon M_0 T R_{\mathcal{A}_2}\sin\beta_2 \tag{8}$$

$$\dot{R_{\mathcal{A}_2}} = -\epsilon\Omega\left(\frac{R_{\mathcal{A}_2}^3}{4} - R_{\mathcal{A}_2}\right) + 2\epsilon R_y(-4A_0\xi\cos\beta_2 + 2A_0\sin\beta_2 + 2A_1\Omega\cos\beta_2) \tag{9}$$

$$\dot{\beta_2} = 2\epsilon\left[-4A_0\epsilon T M_0 + A_0\frac{R_y}{R_{\mathcal{A}_2}}(4\xi\sin\beta_2 + 2\cos\beta_2 - T_2A_1\Omega\sin\beta_2)\right] + \frac{4\Omega^2-1}{2} + \epsilon T M_0\frac{R_{\mathcal{A}_2}}{R_y}\cos\beta_2 \tag{10}$$

4. Model verification

When VIV develops to the steady state, the rate of change of the amplitudes and phase difference becomes zero. At this point, the steady-state amplitude of the structure can be obtained from Eq. 5 – Eq. 10. The obtained steady-state amplitudes are used to identify the structural VIV amplitudes under different Sc numbers in Fig.1. The genetic algorithm (GA) and the nonlinear least-squares algorithm are employed to identify four distinct aerodynamic parameters and three parameters characterizing the fluid-structure coupling effect of the subharmonic wake. The amplitude from Eq.5-Eq.7 is applied to main lock-in range to get four aerodynamic parameters and based on the identified aerodynamic parameters, the other three parameters by the amplitude is obtained from Eq.8-Eq.10. The subharmonic lock-in range can then be determined using the same aerodynamic parameters as those for the main lock-in range. The identified paramsters can be seen in Table 1.

Table 1 The identified parameters

Sc	f_m	L^*	C_{L0}	C_D	T	T_1	T_2
1.9	0.655	1.353	0.021	0.516	0.732	6.165	4.359
3.3	1.658	2.619	0.063	1.587	0.756	5.782	4.257
6	1.776	1.761	0.075	1.563	0.696	6.280	4.529
8.7	2.088	1.840	0.091	1.657	0.727	3.002	4.037
13	3.979	1.300	0.208	4.878	0.131	5.285	5.691
21.7	4.041	2.104	0.197	5.000	0.020	3.008	9.902
38.7	4.013	2.687	0.139	2.169	0.074	5.309	9.870
54.4	5.376	2.721	0.168	4.717	0.058	3.906	9.975

78.1	5.597	2.407	0.151	0.995	0.045	3.257	9.777

Using the paramters in the Table.1, the main lock-in range and the subharmonic lock-in range can be simulated accurately. The model effect can be seen in Fig.2. which describes the amplitudes under different wind speed ratios. It can be observed that as the Sc number increases, the damping effect of the structure is enhanced, and the amplitude of the main resonance decreases, which in turn causes the amplitude of the subharmonic resonance to decline and eventually disappear. Overall, the model exhibits good adaptability to different Sc numbers and achieves favorable simulation performance.

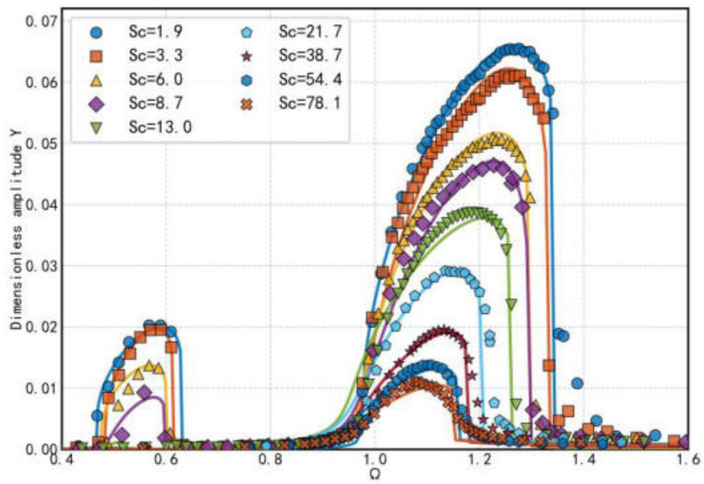

Figure 2 Fitting curve of the theoretical model under the different Sc

5. Conclusion

A subharmonic wake oscillator model is proposed for the subharmonic vibration phenomenon in nonlinear VIV. Using the same aerodynamic parameters as those of the main wake oscillator model, this model can successfully reproduce the 1:2 subharmonic VIV phenomenon. The effectiveness of the model is verified by fitting against wind tunnel test results.

ACKNOWLEDGEMENTS

The authors gratefully acknowledge the support of the National Natural Science Foundation of China (Grant No. 52478552), the Natural Science Foundation of Shanghai (Grant No. 23ZR1464900), and the Fundamental Research Funds for the Central Universities (Grant No. 22120240363).

REFERENCES

Li, J., Wu, P., Hao, J. M., Pan, H. (2022). Experimental and numerical studies on the two "lock-in" regions characteristic of vertical vortex-induced vibration of Π-shaped composite bridge deck. Journal of Wind Engineering and Industrial Aerodynamics 228, 105122.

Marra, A. M., Mannini, C., Bartoli, G. (2015). Measurements and improved model of vortex-induced vibration for an elongated rectangular cylinder. Journal of Wind Engineering and Industrial Aerodynamics 147, 358–367.

Rigo, F., Andrianne, T., Denoël, V. (2022). Parameter identification of wake-oscillator from wind tunnel data. Journal of Fluids and Structures 109, 103474.

Shang, C. J., Xiang, H. Y., Bao, Y. L., Li, Y. L., Luo, K. (2024). Mechanism of vortex-induced vibration in two lock-in regions for truss girder sections. Journal of Wind Engineering and Industrial Aerodynamics 255, 105946.

Zhao, L., Cui, W., Shen, X. M., Xu, S. Y., Ding, Y. J., Ge, Y. J. (2022). A fast on-site measure-analyze-suppress response to control vortex-induced-vibration of a long-span bridge. Structures 35, 192–201.